The severity of phenotype linked to SUCLG1 mutations could be correlated with residual amount of SUCLG1 protein

Cécile Rouzier, Sandie Le Guédard-Méreuze, Konstantina Fragaki, Valérie Serre, Julie Miro, Sylvie Tuffery-Giraud, Annabelle Chaussenot, Sylvie Bannwarth, Céline Caruba, Elsebet Ostergaard, et al.

The severity of phenotype linked to *SUCLG1* mutations could be correlated with residual amount of SUCLG1 protein

Cécile Rouzier,[1,2] Sandie Le Guédard-Méreuze,[3] Konstantina Fragaki,[1,2] Valérie Serre,[4] Julie Miro,[3] Sylvie Tuffery-Giraud,[3] Annabelle Chaussenot,[1] Sylvie Bannwarth,[1,2] Céline Caruba,[5] Elsebet Ostergaard,[6] Jean-François Pellissier,[7] Christian Richelme,[8] Caroline Espil,[9] Brigitte Chabrol,[10] Véronique Paquis-Flucklinger,[1,2]

[1]Department of Medical Genetics, Archet 2 Hospital, CHU of Nice, France.
[2]IGMRC, FRE CNRS / UNSA 3086, Nice Sophia-Antipolis University, France.
[3]Université Montpellier 1, UFR médecine, Montpellier, F-34000, France.
[4]INSERM U781, Necker Enfants Malades Hospital, Paris, France.
[5]Department of Biochemistry, Pasteur Hospital, CHU of Nice, France.
[6]Department of Clinical Genetics, National University Hospital Rigshospitalet, Copenhagen, Denmark
[7]Department of Neuropathology, Timone hospital, CHU of Marseille, France
[8]Department of Pediatrics, Archet 2 Hospital, CHU of Nice, France.
[9]Department of Neuropediatrics, CHU Pellegrin, Bordeaux, France
[10]Department of Neuropediatrics, Timone hospital, CHU of Marseille, France

Running title: Phenotypes linked to *SUCLG1* mutations

To whom correspondence should be addressed:

Pr. Véronique Paquis-Flucklinger
IGMRC, FRE CNRS / UNSA 3086,
Medicine School, 28 av de Valombrose,
06107 Nice cedex 2, France.
Tel: (33) 4 93 37 77 10
Fax: (33) 4 93 37 70 33
e-mail: paquis@hermes.unice.fr

Key words: respiratory chain defect, mtDNA depletion, methylmalonic aciduria, *SUCLG1* mutation, minigene expression system

Word count: 3251 words

Competing interest: None to declare

Abstract

Succinate-CoA ligase deficiency is responsible for encephalomyopathy with mitochondrial DNA depletion and mild methylmalonic aciduria. Mutations in *SUCLA2*, the gene encoding a β subunit of succinate-CoA ligase, have been reported in 17 patients until now. Mutations in *SUCLG1*, encoding the α subunit of the enzyme, have been described in two pedigrees only. We report two unrelated patients harboring three novel pathogenic mutations in *SUCLG1*. The first patient had a severe disease at birth. He was compound heterozygous for a missense mutation (p.Pro170Arg) and a c.97+3G>C mutation which leads to the complete skipping of exon 1 in a minigene expression system. The involvement of *SUCLG1* was confirmed by western blot analysis, which showed absence of SUCLG1 protein in fibroblasts. The second patient has a milder phenotype, similar to that of patients with *SUCLA2* mutations, and is still alive at 12 years of age. Western blot analysis showed some residual SUCLG1 protein in the patient's fibroblasts. Our results suggest that *SUCLG1* mutations that lead to complete absence of SUCLG1 protein are responsible for a very severe disorder with antenatal manifestations, whereas a *SUCLA2*-like phenotype is found in patients with residual SUCLG1 protein. Furthermore, we show that in the absence of SUCLG1 protein, no SUCLA2 protein is found in fibroblasts by western blot analysis. This result is consistent with a degradation of SUCLA2 when its heterodimer partner, SUCLG1, is absent.

Introduction

The mtDNA depletion syndromes (MDS) are a heterogeneous group of severe mitochondrial disorders of infancy and childhood, resulting from a decrease in mtDNA copy number in affected tissues [1-3]. They are inherited as autosomal recessive traits. To date, eight genes have been involved in MDS which can be classified in two genetic categories, those that affect mtDNA replication and those that affect the mitochondrial nucleotide pool [4-11]. Mutations in the *SUCLA2* and *SUCLG1* genes have been found in MDS associated with encephalomyopathic presentations, moderate methylmalonic aciduria [12, 13] and succinate-CoA ligase (SUCL) deficiency. SUCL is an enzyme located in the mitochondrial matrix, composed of an α subunit encoded by *SUCLG1* and a β subunit encoded by either *SUCLA2* or *SUCLG2*, resulting in an ATP-specific SUCL (A-SUCL) and a GTP-specific SUCL (G-SUCL) respectively. A-SUCL and G-SUCL are supposed to catalyse the reversible conversion of succinyl-CoA and ADP or GDP to succinate and ATP or GTP in the Krebs cycle [14]. Several studies have demonstrated that SUCL forms a complex with nucleoside diphosphate kinase (NDPK), which is involved in the salvage of deoxyribonucleotides [15]. An absence of interaction with SUCL could lead to a decreased activity of NDPK and explain the mtDNA depletion observed in SUCL deficiency [16].

To date, mutations in *SUCLA2* have been identified in 12 families, including 8 families of the Faroe islands who have a common ancestor [12, 17, 18]. Most patients were normal at birth but later developed a Leigh-like disorder with dystonia and hearing impairment [19]. Only four patients have been reported with *SUCLG1* mutations. In one pedigree, the three patients carried a homozygous 2 bp deletion [13]. They had a severe lactic acidosis at birth and died within 2-4 days, suggesting that MDS linked to *SUCLG1* mutations are more severe than those caused by *SUCLA2* mutations. Recently though, an additional patient with a

homozygous missense mutation in *SUCLG1* who presented with a milder phenotype, similar to that of patients with *SUCLA2* mutations, was reported [20].

In this study, we describe two unrelated patients harboring novel pathogenic mutations in *SUCLG1* and suggest that the severity of the phenotype is modulated by the presence of a residual amount of SUCLG1 protein.

Patients and methods

Patients

Patient 1 was the second child of unrelated healthy parents. Pregnancy and birth were unremarkable. At age 1 day, he was admitted to intensive care unit with severe hypotonia, respiratory failure and hypoglycemia. Laboratory investigations revealed a lactic acidosis (blood pH 6.76, normal 7.4; HCO_3^- 4.8mmol/l, normal>18 mmol/l; plasma lactate concentration of up to 11.31mmol/l, normal<2.20mmol/l) and a high lactate/pyruvate ratio (33, normal<18). Lactate concentration in cerebrospinal fluid was elevated (22.68mmol/l, normal<3.10mmol/l). Measurement of acylcarnitine esters in plasma revealed increased levels of C3-carnitine (7.5µmol/l, normal<1µmol/l) and C4-dicarboxylic acylcarnitine, which reflect an elevated excretion of methylmalonic acid. The brain magnetic resonance (MR) imaging showed symmetric T2-hyperintense lesions of the basal ganglia and MR spectroscopy in single-voxel revealed a significant elevated lactate doublet peak within abnormal white matter (Fig.1). At age 7 months, psychomotor development was severely delayed with no head control, severe axial hypotonia and poor spontaneous movements. He presented with recurrent episodes of acidosis and respiratory failure. He died at age one year.

Patient 2 was the second son of unrelated healthy parents. Pregnancy and birth were unremarkable. At 3 months of age, he presented with severe hypotonia, feeding difficulties and failure to thrive. Metabolic findings were similar to those of the first patient (lactic acidosis and moderate excretion of methylmalonic acid). At 14 months of age, he presented

with severe psychomotor retardation with lack of head control and sitting posture. Brain magnetic resonance imaging (MRI) is shown in figure 1. At present, he is 12 years old. Clinical examination shows an extremely severe axial hypotonia with no active movements and very atrophic muscles. The patient is tube-fed through a percutaneous endoscopic gastrostomy and he needs permanent respiratory support by tracheotomy.

OXPHOS spectrophotometric measurements

Spectrophotometric studies of OXPHOS complexes and citrate synthase were performed on fibroblasts and muscle crude homogenates, as previously described [21, 22].

Western blotting

50 µg of total protein extracts, obtained as previously described [6], were separated on an acrylamide gel by SDS-PAGE and transferred to a PVDF membrane (Millipore, Saint-Quentin, France). Different primary antibodies have been used. A cocktail of anti-human total OXPHOS complex antibodies (Mitosciences, Eugene, USA) was used at 1/1000. For detection of the SUCLG1 protein, a rabbit polyclonal antibody was used at 1/1000 [13]. For SUCLA2 detection, a rabbit polyclonal antibody against amino acids 53-348 was used at 1/200 (Santa Cruz Biotechonology). Beta-tubulin detection was performed with a mouse monoclonal antibody at 1/10000 (Sigma-Aldrich, St Louis, USA). Anti-rabbit HRP-conjugated secondary antibody was used at 1/20000 and signals were detected using an Enhanced Chemiluminescence system (ECL Plus, Amersham, Piscataway, USA).

Mitochondrial DNA analysis

Blood and tissue samples were obtained after parents had given informed consent. Mitochondrial DNA quantification in muscle was performed by real-time quantitative PCR adapted from the method described by Sarzi *et al*. [23]. Primers and conditions are available on request.

Sequencing of SUCLG1, SUCLA2, SUCLG2 and NME4

The coding exons of *SUCLG1* (NM_003849.2), *SUCLA2* (NM_003850.2), *SUCLG2* (NM_003848.2) and *NME4* (NM_005009.2) genes were amplified with intronic primers by using standard conditions (primers and PCR conditions are available on request). PCR products were purified with ExoSAP-IT enzyme (USB, Cleveland, Ohio, USA), processed with an ABI PRISM® dRhodamine Terminator Cycle Sequencing Ready Reaction kit (Applied Biosystems, Foster City, CA, USA) and analyzed on an ABI 3130 automated sequencer (Applied Biosystems).

PCR-RFLP analysis.

We searched for the presence of the c.509C>G mutation in 360 control chromosomes by PCR-RFLP analysis. This mutation abolishes an *ApaI* restriction site in exon 4 which was amplified with a forward primer in intron 3 : 5'-TGTCCTTTTCTTACCCCAAGA-3' and a reverse primer in intron 4 : 5'-GAGTTTTGAGGGTTTAAGGCA-3'. After *ApaI* digestion, 2 fragments of 292 and 280 bp are found in wild-type PCR controls. The 572 bp PCR fragment is not digested when the c.509C>G mutation is present.

In silico analysis

The model (residues 41 to 346) was obtained by comparative protein modeling methods and energy minimization using the Swiss-Model program. The 2.96 Å coordinate set for the pig enzyme in complex with GDP (pdb code 2fpg) was used as a template for modeling the human enzyme. Swiss-pdb Viewer 3.7 (http://www.expasy.org/spdbv) was used to analyze and visualize the structures.

RT-PCR analysis

Total RNA were extracted by using the Trizol reagent (Invitrogen, Carlsbad, CA) according to the manufacturer's instructions. cDNA synthesis and PCR amplifications were performed using the SuperScript One-Step kit, RT-PCR with Platinum Taq (Invitrogen). Reverse

transcription consisted of one cycle at 55°C for 30 min and 94°C for 2min and was followed by PCR amplification (primers and PCR conditions are available on request).

Ex vivo splicing assay

An overlap extension PCR strategy [24] was used, due to the large size of *SUCLG1* intron 1 (9.4 kb), to construct a chimeric minigene assembling *SUCLG1* exon 1 with its upstream (498 bp) and downstream (173 bp) intronic sequences (fragment 1) and exon 2 with its flanking intronic sequences (406 bp of intron 1 and 146 bp of intron 2) (fragment 2). The PCRs were performed from the genomic DNA of patient 1 using the Hot Start High Fidelity Phusion polymerase (Finnzymes). Sequences of primers are available upon request. The final full-length product (1617 bp) was inserted between the XhoI/NheI restriction sites of the pcDNA3.1(+) mammalian expression vector (Invitrogen) using the T4 DNA ligase (Invitrogen) and validated by direct sequencing. Transient transfections in HeLa cells were carried out in 6-well plates using 6 µl of FuGENE6 (Roche) and 1 µg of wild-type or mutated minigene constructs according to the manufacturer's instructions. Experiments were carried out in triplicate and in at least two independent transfections. Cells were harvested 48 h post transfection. Total cytoplasmic RNA was extracted using the Nucleospin RNAII Kit (Macherey-Nagel). First-strand cDNA synthesis was performed from 1 µg of total RNA, with random hexamers as primers (Invitrogen) and Superscript II (Invitrogen). One tenth of the synthesized cDNA was used as a template for the subsequent PCR with the T7 forward vector specific primer and a gene-specific reverse primer (5'-CTGTTTGCCAGTGAAACCCTGG-3'). Amplification was performed using the Hot Start High Fidelity Phusion polymerase (Finnzymes) for 35 cycles, consisting of 10 sec at 98°C, 20 sec at 53°C and 50 sec at 72°C. The products were resolved on 1.5% agarose gel. All PCR products were confirmed by DNA sequencing.

Results

Patient 1

Histological analysis of the muscle tissue showed intracellular lipid accumulation with numerous cox-negative and a few ragged-red fibers (not shown). Enzymatic spectrophotometric measurements of the individual respiratory chain complexes in muscle revealed a decrease of complex I, II, IV and V activity (Table 1A). Additionally, all activity ratios compared to complex IV, which best reflect the balanced respiratory enzyme activity [25], were severely abnormal in muscle. In fibroblasts, the specific activities of complex II, III, and IV were also decreased with an imbalance in the ratios between the complexes (Table 1B).

Table 1A

MUSCLE BIOPSY						
OXPHOS complexes	*I*	*II*	**III**	**IV**	*V*	*CS*
Control values (nmol/min/mg of proteins)	10-32	20-65	94-236	89-347	32-89	82-234
Patient	**6.9**	**15.2**	157.9	**21.3**	**24.2**	107.2
Ratios	*IV / I*	**IV / II**	**IV / III**	**IV / V**	**IV / CS**	
Control values	5.54-21.20	3.20-7.90	1-2	2.59-5.40	1.01-2.16	
Patient	**3.08**	**1.40**	**0.13**	**0.88**	**0.19**	

Table 1B

FIBROBLASTS						
OXPHOS complexes	*I*	*II*	**III**	**IV**	*V*	*CS*
Control values (nmol/min/mg of proteins)	9.0-27.1	8.6-20.2	57.4-176.2	109.9-252.7	22.0-46.2	74.7-161.1
Patient	11.6	**7.5**	**47.9**	**78.1**	37.6	116.6
Ratios	*IV / I*	**IV / II**	**IV / III**	**IV / V**	**IV / CS**	
Control values	5.02-21.78	6.38-24.65	0.98-3.76	2.83-7.98	1.04-2.71	
Patient	6.73	10.41	1.63	**2.07**	**0.67**	

In agreement with the enzyme measurements, western blot analysis demonstrated a marked reduction in the amount of specific proteins of complexes I, II, III and IV in patient's fibroblasts compared to control (Fig. 2A). Muscle was not available for western blotting

analysis. The relative mtDNA copy number showed a decreased amount of mtDNA in muscle (11% of age-matched controls).

The clinical presentation including encephalomyopathy with mtDNA depletion and mild methylmalonic aciduria led us to perform mutation screening of genes involved in succinate-CoA ligase. No mutation was found in *SUCLA2*. Mutation analysis of the *SUCLG1* gene showed that the patient was compound heterozygous for 2 novel mutations: c.509C>G (p.Pro170Arg) and c.97+3G>C (Fig. 2B). The involvement of *SUCLG1* was confirmed by western blotting analysis which showed a total absence of SUCLG1 protein in patient's fibroblasts (Fig. 2C).

The c.509C>G mutation was inherited from the mother, and the healthy older sister was also heterozygous for the mutation. The missense mutation changes a highly conserved neutral proline into a polar charged basic arginine and was not found in 360 healthy French control chromosomes (Fig. 2D). The p.Pro170Arg mutation maps within the CoA-ligase domain and we carried out prediction studies of putative impact on SUCL-G structure and function. The high degree of identity (96%) between the pig GTP-specific succinyl CoA synthetase and SUCL-G α-subunits prompted us to predict the three-dimensional structure of the human enzyme. The missense mutation p.Pro170Arg is localized close to the catalytic histidine residue and the CoA-binding domain. The putative creation of an ionic bound with one of the neighbouring acidic residues could alter the flexibility of the loop connecting the two domains of the α-subunit (Fig. 3).

The second mutation c.97+3G>C, inherited from the father changes the highly conserved G nucleotide at position +3 of the donor splice site (5'ss) in intron 1. This base substitution was predicted to drastically decrease the intrinsic strength of this 5'ss by using three different splice-site prediction algorithms (MaxEntScan available at http://genes.mit.edu/burgelab/maxent/Xmaxentscan_scoreseq.html, Splice-site Neural

Network algorithm (SSPNN: NNSPLICE 0.9 version) available at http://www.fruitfly.org and SpliceSiteFrame available at http://ast.bioinfo.tau.ac.il/SpliceSiteFrame.htm). We first attempted to characterize the splicing outcome of this sequence variation by RT-PCR analysis from patient's fibroblasts, with a forward primer in exon 1 and a reverse primer in the last exon of *SUCLG1* (exon 9). No aberrantly spliced mRNA could be identified and sequence analysis of the RT-PCR reaction detected only one allele with the 509 C to G mutation. Hence we designed a splicing reporter minigene containing exon 1 and exon 2 of *SUCLG1* with part of their flanking intronic sequences, containing a strong cryptic 5'ss predicted by the Human Splicing Finder (HSF) tool (http://www.umd.be/HSF/) which was located 314 bp upstream exon 1, to perform an *ex vivo* splicing assay (Fig. 4A). After transfection into HeLa cells, the effects on splicing were evaluated by RT-PCR analysis and systematic sequencing. No transcript retaining exon 1 could be detected in presence of the mutation. Indeed, the mutant minigene disclosed only a short fragment resulting from the complete skipping of exon 1 by the occurrence of a splicing event between the upstream cryptic 5'ss together with the acceptor splice site (3'ss) in intron 1 (Fig. 4A). In the wild-type context, two transcript species were detected. In both transcripts, the cryptic 5'ss was used either in combination with the 3'ss in intron 1 (transcript missing exon 1) as observed in the mutant or with a new cryptic exonic 3'ss (MaxEntScan score, 4.97) located 5 base pairs downstream of the established 5' border of exon 1 (transcript including exon 1) which preserves the translation initiation site (Fig. 4A). To further investigate *in vivo* the functionality of the two newly identified 5'ss and 3'ss, we performed a new RT-PCR analysis from both patient and control fibroblasts with a forward primer located upstream the cryptic 5'ss sequence. As observed in the wild-type construct, we confirmed the presence of two *SUCLG1* mRNA isoforms in control fibroblasts resulting from alternative splicing of exon 1. Both isoforms contain an exonic sequence, upstream of exon 1, bound either to exon 1 (use of the cryptic exonic 3'ss) or to exon 2 (Fig.

4B). The same transcripts were found in patient's fibroblasts because of the presence of the wild-type allele. Hence we have evidenced the presence of a so-far unreported exonic sequence upstream of *SUCLG1* exon 1, which is likely untranslated when bound to exon 1. We have found a cDNA sequence corresponding to the second isoform lacking exon 1 in databases (BU600891; www.genome.ucsc.edu; www.ensembl.org). Nevertheless, the role of the putative corresponding gene product, which lacks the initiation AUG codon and the mitochondrial targeting sequence, has to be determined.

Patient 2

At 2 years of age, analysis of muscle showed numerous cox-negative fibers and lipid accumulation (not shown). On electron microscopy, abnormal enlarged mitochondria contained lipid droplets (Fig. 5A). Enzymatic spectrophotometric measurements showed markedly reduced activities for complexes I and IV (not shown) and we found a mtDNA depletion (18% of age-matched controls). No mutation was identified by sequencing the *SUCLA2* gene. Mutation analysis of *SUCLG1* showed that the patient was heterozygous for a c.448C>T (p.Gln150X) mutation (Fig. 5B), which was inherited from his healthy mother. We failed to identify a second mutation by *SUCLG1* sequencing. Furthermore, we did not detect any sequence variation by sequencing the complete cDNA from fibroblasts. Immunoblot analysis of fibroblasts showed a decreased amount of SUCLG1 protein in patient compared with controls (Fig. 5C).

A-SUCL is a heterodimer composed of SUCLG1 and SUCLA2. We looked at the expression of SUCLA2 protein in our patients harboring SUCLG1 deficiencies. Western blotting in fibroblasts of patient 1, who harbors a complete absence of SUCLG1 protein, showed no expression of the *SUCLA2* gene product (Fig. 5D). On the contrary, we only found a decreased amount of SUCLA2 when a residual amount of SUCLG1 protein is present (patient 2). These results are consistent with a destabilization of SUCLA2 in the absence of its

heterodimer partner, SUCLG1.

Discussion

The first patients described with *SUCLG1* mutations had a very severe phenotype at birth with death during the first days of life [13]. Patients with *SUCLA2* mutations had a milder phenotype. They were generally normal at birth and later developed psychomotor retardation, severe muscle hypotonia, hyperkinetic movement disorders and sensorineural deafness [12 18 17]. Recently, Ostergaard *et al*. described a patient with *SUCLG1* mutations, presenting with a phenotype similar to that of patients with *SUCLA2* mutations. Our patient 1 had a complete absence of SUCLG1 protein in fibroblasts. He presented with severe hypotonia and lactic acidosis at birth. He developed psychomotor development with recurrent episodes of acidosis leading to death at one year of age. Our patient 2 had a residual amount of SUCLG1 in fibroblasts. The first symptoms appeared at 3 months of age and he is still alive at 12 years of age. Similarly, Ostergaard *et al.* described a severe disease in patients showing a complete absence of SUCLG1 while the patient who expressed small amount of SUCLG1 protein presented with a "SUCLA2-like" phenotype [13, 20]. All together, these results suggest that the severity of the phenotype is modulated by a residual amount of SUCLG1 enzyme. Furthermore, we show that in fibroblasts a complete absence of SUCLG1 likely leads to degradation of SUCLA2, its heterodimer partner. It is reasonable to assume that an extremely severe phenotype with antenatal manifestations is observed when the absence of SUCLG1 leads to a complete abolition of both G-SUCL and A-SUCL activities. In patients with *SUCLA2* mutations or *SUCLG1* mutations that do not fully abolish SUCLG1 expression, some residual SUCL activity is present and the interaction with NDPK could be conserved thus NDPK activity.

Brain imaging in most patients with *SUCLA2* mutations showed basal ganglia involvement closely resembling Leigh syndrome [12, 18 17]. Brain MRI data were available for only one

patient with *SUCLG1* mutations showing findings similar to that of patients with *SUCLA2* mutations [20]. Our *SUCLG1* patients also showed basal ganglia abnormalities. In addition, we found in both patients bilateral and symmetrical white matter involvement, which has not been reported previously. Albeit, neuroimaging of only a few patients has been reported, it does not seem to be associated with mutations in a specific gene and both *SUCLA2* and *SUCLG1* genes have to be tested in patients with encephalomyopathic presentations associated with mild methylmalonic aciduria.

We have strong arguments for the pathogenicity of the three novel mutations that we detected. In patient 1, p.Pro170Arg affects highly conserved residue during evolution and was not found in 180 controls. Its location within the CoA-ligase domain and the prediction studies of its putative impact on SUCL-G structure and function are in favor of a deleterious effect. Indeed, this mutation may induce a local conformational change, altering the flexibility, proper interface interactions and ligand binding. In a more dramatical way, the p.Pro170Arg mutation may completely disrupt the local tertiary structure of the protein leading to a wrong folding which would explain why the protein is unable to form a complex with the β subunit. The second heterozygous mutation in patient 1, c.97+3G>C, was predicted to affect the 5'ss in intron 1. By using an *ex vivo* splicing assay, we demonstrated that this variant results in the skipping of exon 1 in all transcripts leading to the loss of the AUG initiation codon and the mitochondrial targeting sequence located in the first 40 amino acids of the SUCLG1 protein. Both *ex vivo* and *in vivo* assays on control fibroblasts showed the inclusion of an exonic sequence upstream of the exon 1 in the *SUCLG1* transcripts, the role of which remains to be determined. Combined with the results of the immunoblot analysis showing the complete absence of SUCLG1 protein in the patient's fibroblasts, we demonstrate that the identified mutations result in the absence of a functional protein.

The heterozygous nonsense mutation p.Gln150X in patient 2 is expected to lead to the synthesis of a truncated protein which lacks the CoA-ligase domain. Unfortunately, we failed to identify a second mutation in *SUCLG1*, but we did not search for large deletions or deep intronic mutations. Sequencing of *SUCLA2*, *SUCLG2* and *NME4* (coding for the mitochondrial NDPK) revealed no mutation. Taken together, these findings and the severe decrease of SUCLG1 protein on immunoblot analysis are in favour of the involvement of *SUCLG1* in the disease.

In conclusion, we confirm the role of *SUCLG1* in encephalomyopathy with mtDNA depletion and mild methylmalonic aciduria. Overlap between the clinical presentations linked to *SUCLG1* or *SUCLA2* mutations should lead to screening of both genes in these phenotypes.

Acknowledgements

We thank Alexia Figueroa for technical help. This work was made possible by grants to V.P-F from the Association Française contre les Myopathies (AFM).

References

1. Suomalainen A, Kaukonen J. Diseases caused by nuclear genes affecting mtDNA stability. *Am J Med Genet* 2001;**106**:53-61.
2. Alberio S, Mineri R, Tiranti V, Zeviani M. Depletion of mtDNA : syndromes and genes. *Mitochondrion* 2007;**7**:6-12.
3. Spinazzola A, Zeviani M. Disorders from perturbations of nuclear-mitochondrial intergenomic cross-talk. *J Intern Med* 2009;**265**:174-192.
4. Copeland W. Inherited mitochondrial diseases of DNA replication. *Ann Rev Med* 2008;**59**:131-146.
5. Saada A, Shaag A, Mandel H, Nevo Y, Eriksson S, Elpeleg O. Mutant mitochondrial thymidine kinase in mitochondrial DNA depletion myopathy. *Nat Genet* 2001;**29**:342-344.
6. Bourdon A, Minai L, Serre V, Jais J, Sarzi E, Aubert S, Chrétien D, de Lonlay P, Paquis-Flucklinger V, Arakawa H, Nakamura Y, Munnich A, Rotig A. Mutation of RRM2B, encoding p53-controlled ribonucleotide reductase (p53R2), causes severe mitochondrial DNA depletion. *Nat Genet* 2007;**39**:776-780.
7. Bornstein B, Area E, Flanigan K, Ganesh J, Jayakar P, Swoboda K, Coku J, Naini A, Shanske S, Tanji K, Hirano M, DiMauro S. Mitochondrial DNA depletion syndrome due to mutations in the RRM2B gene. *Neuromuscul Disord* 2008;**18**:453-459.
8. Mandel H, Szargel R, Labay V, Elpeleg O, Saada A, Shalata A, Anbinder Y, Berkowitz D, Hartman C, Barak M, Eriksson S, Cohen N. The deoxyguanosine kinase gene is mutated in individuals with depleted hepatocerebral mitochondrial DNA. *Nat Genet* 2001;**29**:337-341.

9. Spinazzola A, Viscomi C, Fernandez-Vizzara E, Carrara F, D'Adamo P, Calvo S, Marsano R, Donnini C, Weiher H, Strisciuglio P, Parini R, Sarzi E, Chan A, DiMauro S, Rotig A, Gasparini P, Ferrero I, Mootha V, Tiranti V, Zeviani M. MPV17 encodes an inner mitochondrial membrane protein and is mutated in infantile hepatic mitochondrial DNA depletion. *Nat Genet* 2006;**38**:570-575.
10. Naviaux R, Nguyen K. POLG mutations associated with Alpers' syndrome and mitochondrial DNA depletion. *Ann Neurol* 2004;**55**:706-713.
11. Sarzi E, Goffart S, Serre V, Chrétien D, Slama A, Munnich A, Spelbrink J, Rotig A. Twinkle helicase (PEO1) gene mutation causes mitochondrial DNA depletion. *Ann Neurol* 2007;**62**:579-587.
12. Elpeleg O, Miller C, Hershkovitz E, Bitner-Glindzick M, Bondi-Rubinstein G, Rahman S, Pagnamenta A, Eshhar S, Saada A. Deficiency of the ADP-forming Succinyl-CoA synthase activity is associated with encephalomyopathy and mitochondrial DNA depletion. *Am J Hum Genet* 2005;**76**:1081-1086.
13. Ostergaard E, Christensen E, Kristensen E, Mogensen B, Duno M, Southbridge E, Wibrand F. Deficiency of the alpha subunit of succinate-Coenzyme A ligase causes fatal infantile lactic acidosis with mitochondrial DNA depletion. *Am J Hum Genet* 2007;**81**:383-387.
14. Johnson J, Muhonen W, Lambeth D. Characterization of the ATP- and GTP- specific succinyl-CoA synthetases in pigeon. The enzymes incorporate the same alpha-subunit. *J Biol Chem* 1998;**273**:27573-9.
15. Kowluru A, Tannous M, HQ C. Localizatio and characterization of the mitochondrial isoform of the nucleoside diphosphate kinase in the pancreatic beta cell: evidence for its complexation with mitochondrial succinyl-CoA synthetase. *Arch Bochem Biophys* 2002;**398**:160-169.
16. Ostergaard E. Disorders caused by deficiency of succinate-CoA ligase. *J Inherit Metab Dis* 2008;**31**:226-229.
17. Ostergaard E, Hansen F, Sorensen N, Duno M, Vissing J, Larsen P, Faeroe O, Thorgrimsson S, Wibrand F, Christensen E, Schwartz M. Mitochondrial encephalomyopathy with elavated methylmalonic acid is caused by SUCLA2 mutations. *Brain* 2007;**130**:853-861.
18. Carrozzo R, Dionisi-Vici C, Steuerwald U, Lucioli S, Deodato F, Di Giandomenico S, Bertini E, Franke B, Kluitjmans L, Meschini M, Rizzo C, iemonte F, Rodenburg R, Santer R, Santorelli F, van Rooij A, Koning V-d, Morava E, Wevers R. SUCLA2 mutations are associated with mld methylmalonic aciduria, Leigh-like encephalomyopathy, dystonia and deafness. *Brain* 2007;**130**:862-874.
19. Chinnery P. Mutations in SUCLA2: a tandem ride back to the Krebs cycle. *Brain* 2007;**130**:606-609.
20. Ostergaard E, Schwartz M, Batbayli M, Christensen E, Hjalmarson O, Kollberg G, Holme E. A novel misense mutation in SUCLG1 associated with mitochondrial DNA depletion, encephalomyopathic form with methylmalonic aciduria. *Eur J Pediatr* 2009.
21. Rustin P, Chretien D, Bourgeron T, Gérard B, Rotig A, Saudubray J, Munnich A. Biochemical and molecular investigations in respiratory chain deficiencies. *Clin Chim Acta* 1994;**228**:35-51.
22. Bradford M. A rapid and sensitive method for the quantitation of microgram quantities of protein utilizing the principle of protein-dye binding. *Anal Biochem* 1976;**72**:248-254.

23. Sarzi E, Bourdon A, Chrétien D, Zarhate M, Corcos J, Slama A, Cormier-Daire V, de Lonlay P, Munnich A, Rotig A. Mitochondrial DNA depletion is a prevalent cause of multiple respiratory chain deficiency in childhood. *J Pediatr* 2007;**150**:531-534.
24. Heckman K, Pease L. Gene splicing and mutagenesis by PCR-driven overlap extension. *Nat Protoc* 2007;**2**:924-932.
25. Chretien D, Rustin P, Bourgeron T, Rotig A, Saudubray J, Munnich A. Reference charts for respiratory chain activities in human tissues. *Clin Chim Acta* 1994;**228**:53-70.

Titles and legends to figures

Table 1. Respiratory chain enzyme activities in muscle biopsy (A) and fibroblasts (B) of patient 1. Activities were measured spectrophotometrically. Results are expressed i) as absolute values for controls or patient (in nanomol of substrate per minute per milligram of protein) and ii) as activity ratios compared to complex IV. The abnormal values are in bold.

Figure 1. Brain MR images of patient 1 (A-D) and patient 2 (E-H). A. Axial T1-weighted image revealing slight symmetrical hyperintensities in the posterior lenticular nuclei (arrow) and the limb of internal capsula associated with T1 hypointensities in the frontal periventricular white matter. **B**. Axial diffusion-weighted image showing a decrease of Apparent Diffusion Coefficient in the posterior putamen. **C-D.** Single-voxel MR spectroscopy of the abnormal right parietal white matter revealing a prominent lactate peak which is clearly visible as an inverted doublet (arrow). **E-F.** Axial T2-weighted and FLAIR (FLuid-Attenuated Inversion Recovery) images showing brain atrophy with enlarged sylvian fissures, bilateral and symmetrical atrophy of putamen, caudate nuclei and globi pallidi with high signals on T2-weighted and low signals on FLAIR. **G.** Axial FLAIR image showing symmetrical hyperintensities in middle cerebellar peduncles and dentate nuclei. **H.** Axial T1-weighted image showing symmetrical hypointensities of ventral mesencephalon (corpora quadrigemina).

Figure 2. Identification of novel *SUCLG1* mutations leading to G-SUCL defect in patient 1. A. Western blot analysis of patient's fibroblasts. Equal amounts of proteins from patient 1 (P) and a control subject (C) were subjected to SDS-PAGE and blotted onto a PVDF

membrane prior to incubation with a cocktail of anti human total OXPHOS complexes monoclonal antibodies. **B**. Sequence analysis of *SUCLG1* showing the c.509C>G (upper panel) and the c.97+3G>C (lower panel) mutations. **C.** Western blot analysis of patient's fibroblasts. Equal amounts of proteins from controls (C1 and C2) and patient 1 (P) were subjected to SDS-PAGE and blotted onto a PVDF membrane prior to incubation with antibodies against SUCLG1 (upper panel) and β-tubulin (lower panel). **D**. Alignments of 12 vertebrate amino acid sequences including the proline in position 170 (surrounded by a red rectangle).

Figure 3. Modelled structure of the human SUCLG1 protein. A. The modelled α-subunit of SUCL-G is represented in yellow and green and superimposed with the grey dimeric template (dark grey for the α-subunit and light grey for the β-subunit). Pro170 located in the α-subunit of SUCL-G is shown in red. The pig GTP-specific succinyl-CoA synthetase was co-crystalized with GDP (in magenta), potassium ion (in light blue) and a phosphate ion (in orange). The α-subunit includes a doubly wound parallel β-sheet or nucleotide binding motif ("Rossmann fold"). Interestingly, the missense mutation p.Pro170Arg is localized on a loop linking these two domains and may create an ionic bound with Glu145 (in brown) or Asp229 (in dark blue) close to the mutated residue. **B.** The modelled α-subunit of SUCL-G is represented in yellow and green as in figure 3A, but in another orientation. The *E. coli* succinyl-CoA synthetase (pdb code: 1scu) has been co-crystallized with the coenzyme A (CoA). The α-subunit of *E. coli* enzyme is depicted in grey, and the CoA bound in the N-ter of the α-subunit is shown in blue. The *E. coli* catalytic phosphorylated histidine residue is shown in black and orange.

Figure 4A. *Ex vivo* analysis of the c.97+3G>C mutation. The genomic DNA segment tested is shown schematically above the panel. Black boxes (marked V) represent exons of the splicing reporter minigene. E1, *SUCLG1* exon 1. E2, *SUCLG1* exon 2. I1, *SUCLG1* intron 1.

ss, splice site. Intron sequence is shown in lower case, exon sequence in upper case. The triangle represents the 8841bp deletion in intron 1 made by PCR overlap. Splicing patterns, determined by sequencing each product, are shown schematically alongside the right-hand margin of the gel. M, molecular weight marker. wt, wild-type. m, mutant. (-), negative control without reverse transcriptase. In the mutant, there is a complete abolition of the 5'ss of exon 1 in favor of a cryptic 5'ss, marked gt, upstream of exon 1 and leading to exon 1 skipping. In the wild-type construct, the same cryptic donor site is used either with the 3'ss in intron 1 or with a newly identified cryptic 3'ss at the beginning of exon 1. **B**. ***In vivo*** **analysis of the c.97+3G>C mutation.** The position of the PCR primers used after reverse transcriptase step is indicated in left panel (small arrows). All RT-PCR products shown have been sequenced and their sizes are marked alongside the right-margin of the gels. P, patient. C1, C2 control subjects. bp, base pair. Upper panel, nested PCR performed with a forward primer upstream of the cryptic 5'ss and a reverse primer in exon 1. Middle panel, nested PCR performed with a forward primer in exon 1 and a reverse primer in exon 2. Lower panel, PCR performed with a forward primer upstream of the cryptic 5'ss and a reverse primer in exon 2.

Figure 5A-C. SUCLG1 defect in patient 2. A. Electron micrographs showing abnormal enlarged mitochondria and lipid droplets in muscle fibers. Original magnification, x12000. **B.** Sequence analysis of *SUCLG1* showing the c.448C>T mutation on the non-coding strand. **C.** Western blot analysis of patient's fibroblasts. Equal amounts of proteins from controls (C1 and C2) and patient 1 (P) were subjected to SDS-PAGE and blotted onto a PVDF membrane prior to incubation with antibodies against SUCLG1 (upper panel) and β-tubulin (lower panel). **D. Western blot of SUCLA2 in patients 1 and 2.** Equal amounts of fibroblast proteins from patients (P1 and P2) and controls (C1 and C2) were subjected to SDS-PAGE and blotted onto a PVDF membrane prior to incubation with antibodies against SUCLA2 (upper panel) and β-tubulin (lower panel).

Licence

"The Corresponding Author has the right to grant on behalf of all authors and does grant on behalf of all authors, an exclusive licence (or non exclusive for government employees) on a worldwide basis to the BMJ Publishing Group Ltd to permit this article (if accepted) to be published in JMG and any other BMJPGL products and sublicences such use and exploit all subsidiary rights, as set out in our licence (http://group.bmj.com/products/journals/instructions-for-authors/licence-forms)."

Véronique Paquis (on behalf of all authors)

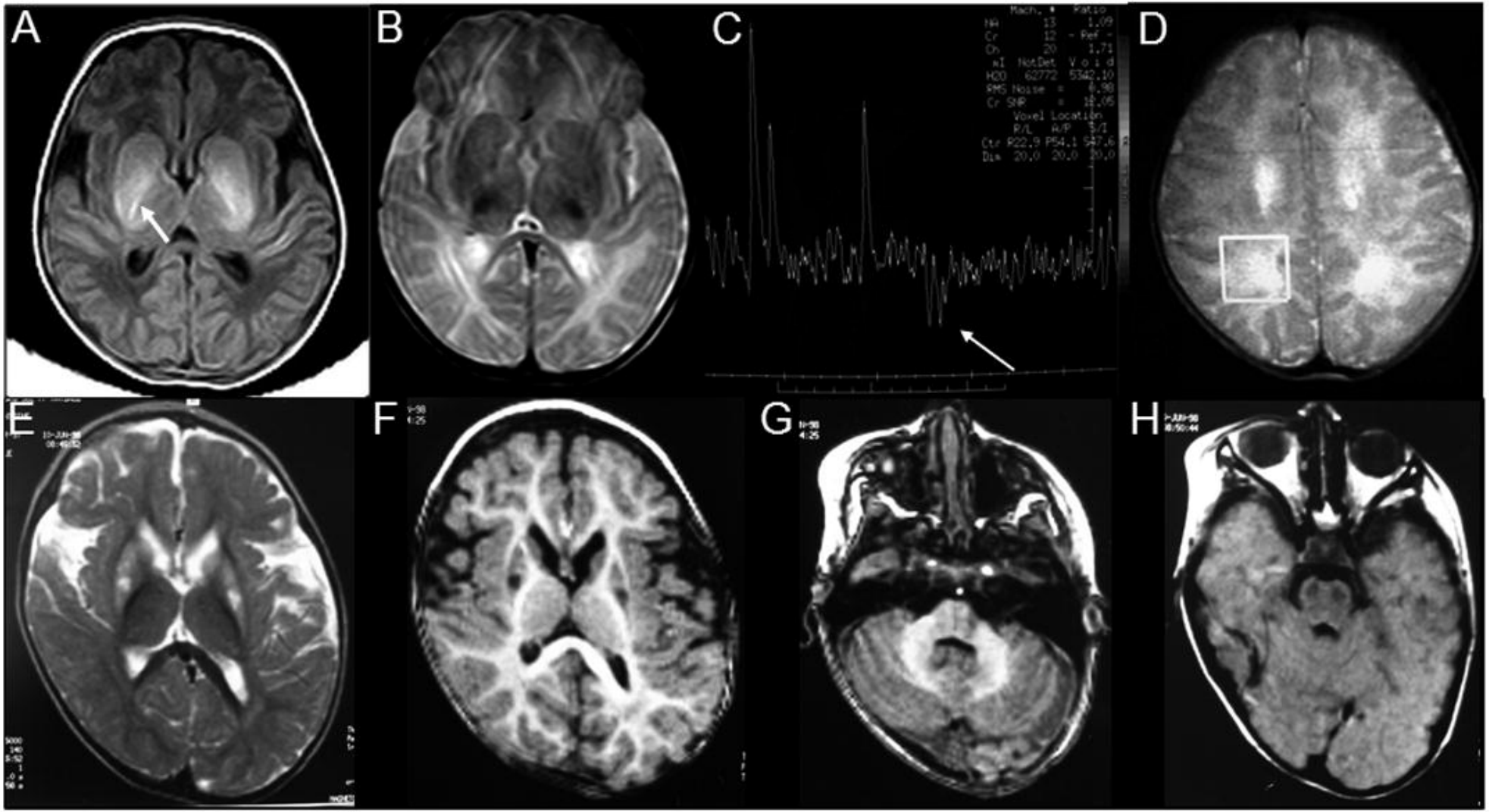

Figure 1

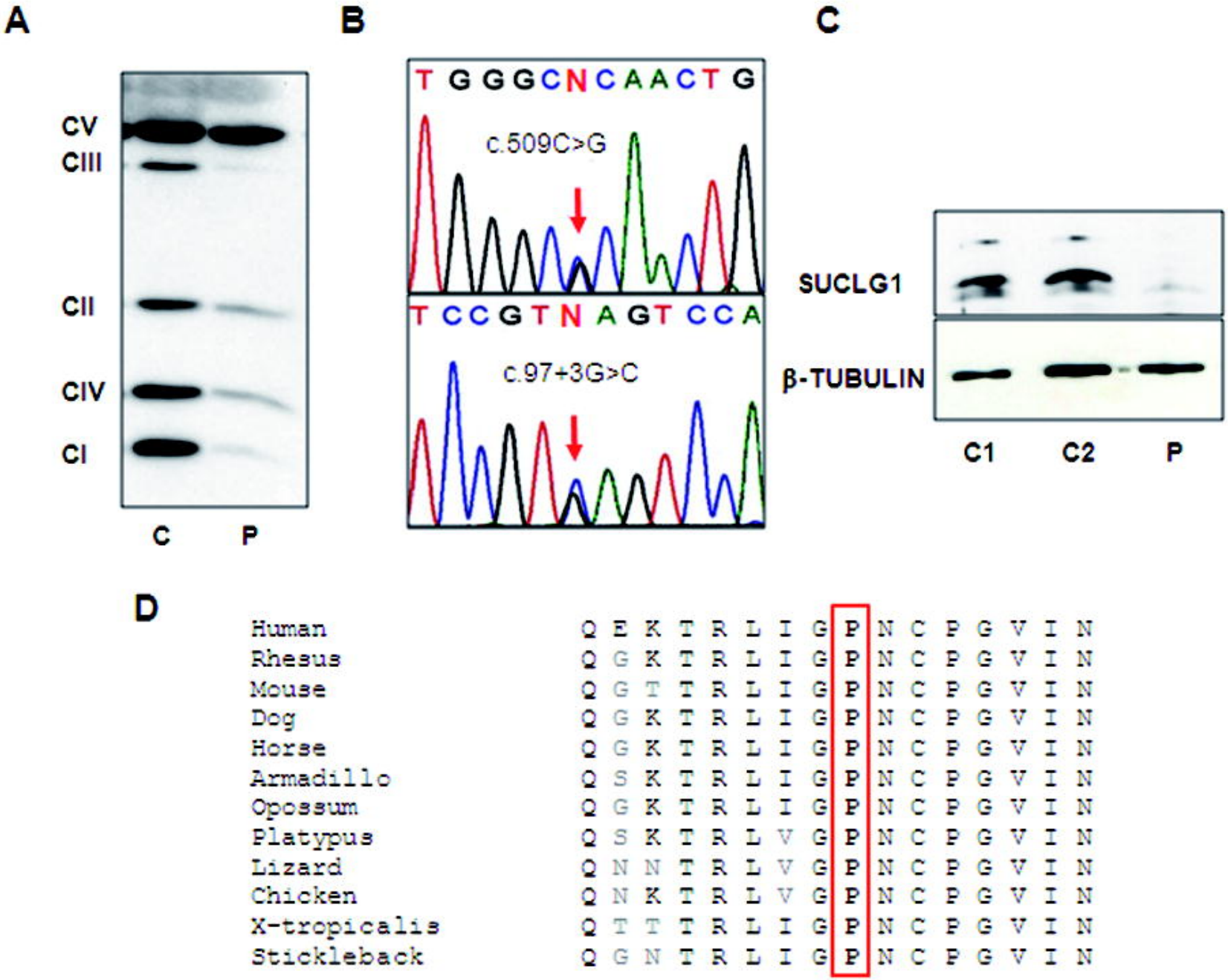
A
CV
CIII
CII
CIV
CI
C
P
B
T G G G C N C A A C T G
c.509C>G
T C C G T N A G T C C A
c.97+3G>C
C
SUCLG1
β-TUBULIN
C1
C2
P
D
Human Q E K T R L I G P N C P G V I N
Rhesus Q G K T R L I G P N C P G V I N
Mouse Q G T T R L I G P N C P G V I N
Dog Q G K T R L I G P N C P G V I N
Horse Q G K T R L I G P N C P G V I N
Armadillo Q S K T R L I G P N C P G V I N
Opossum Q G K T R L I G P N C P G V I N
Platypus Q S K T R L V G P N C P G V I N
Lizard Q N N T R L V G P N C P G V I N
Chicken Q N K T R L V G P N C P G V I N
X-tropicalis Q T T T R L I G P N C P G V I N
Stickleback Q G N T R L I G P N C P G V I N

Figure 2

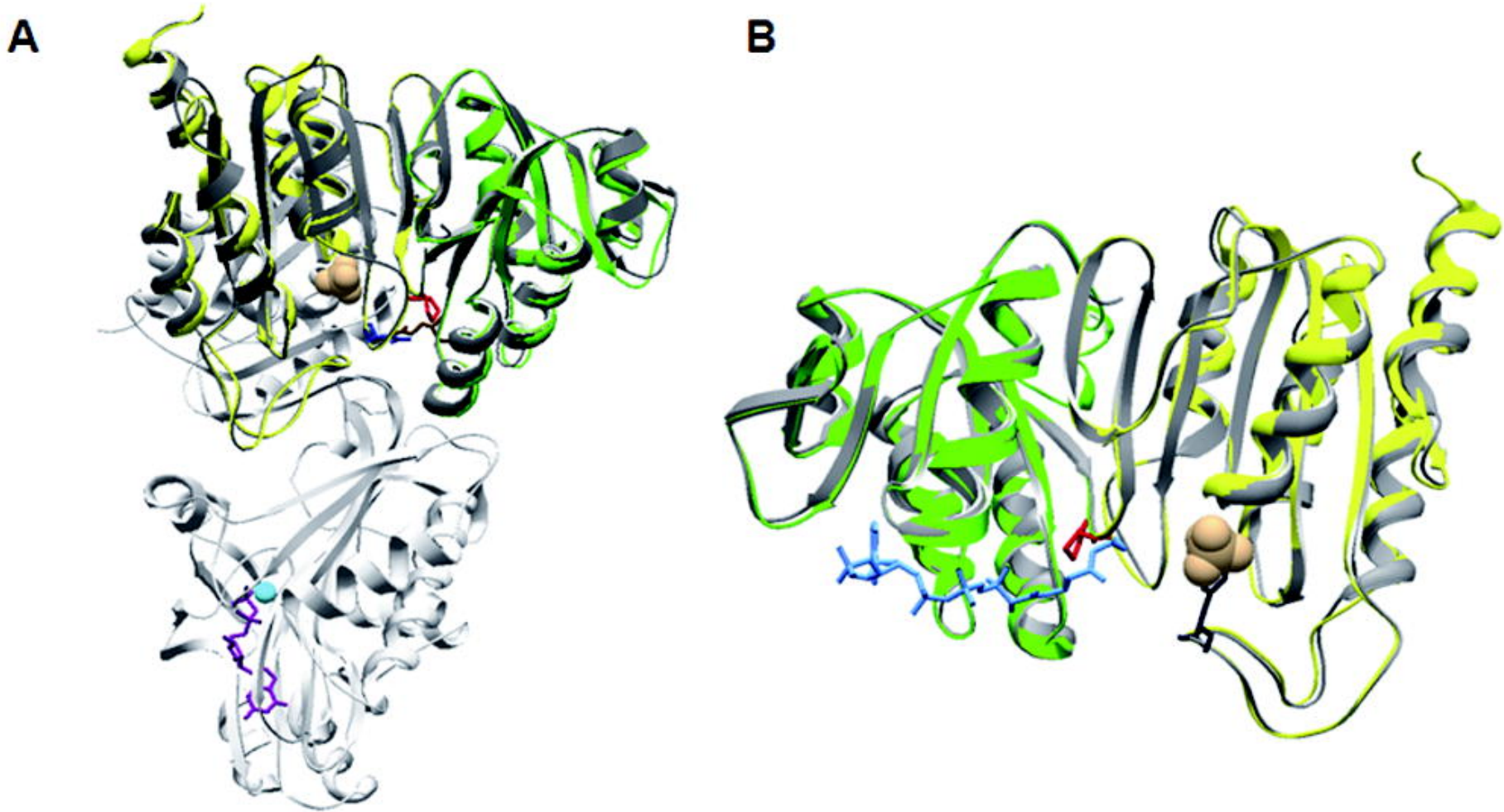

Figure 3

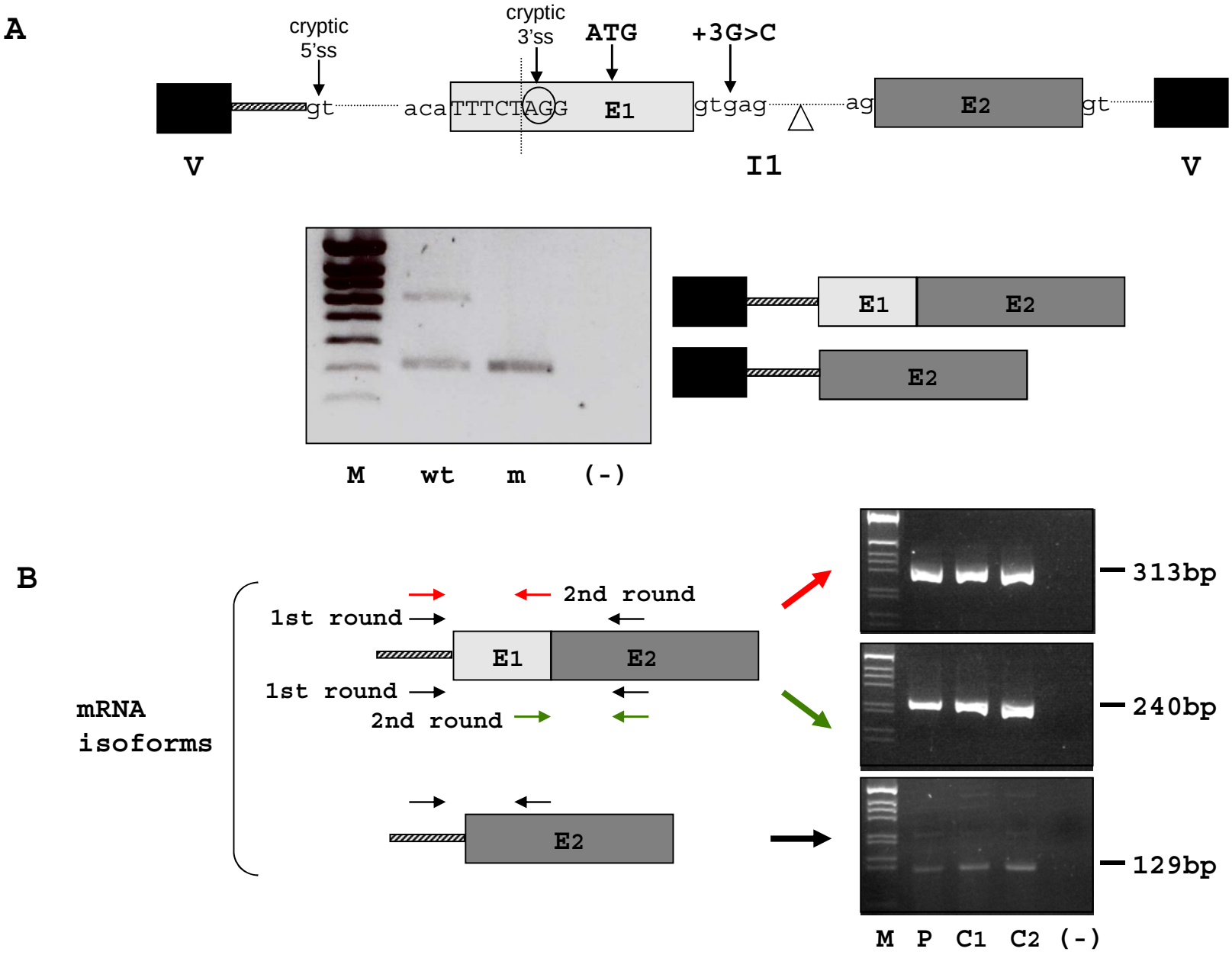
A
cryptic
5'ss
cryptic
3'ss
ATG
+3G>C
gt
acaTTTCTAGG
E1
gtgag
ag
E2
gt
V
I1
V
M
wt
m
(-)
E1
E2
E2
B
mRNA
isoforms
1st round
2nd round
E1
E2
1st round
2nd round
E2
313bp
240bp
129bp
M
P
C1
C2
(-)

Figure 4

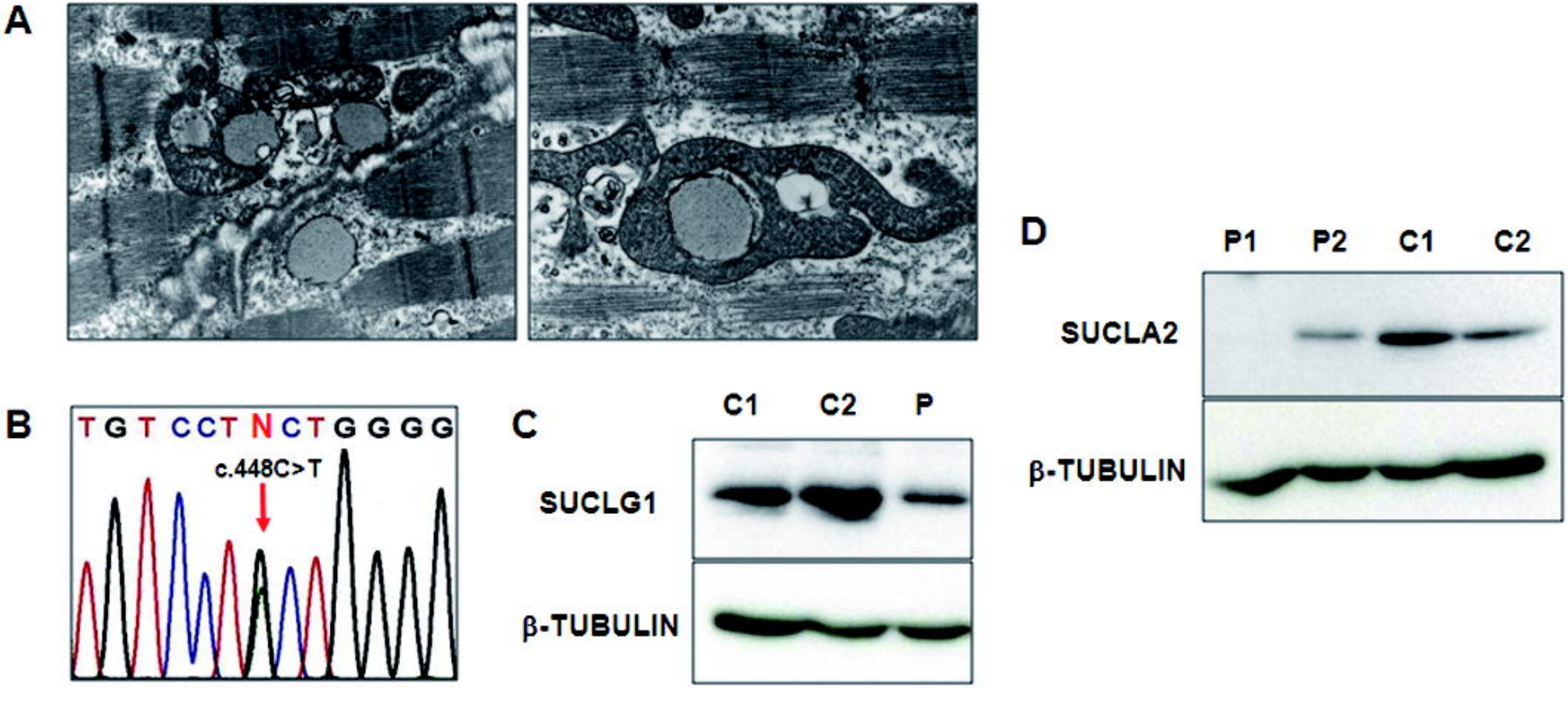
A
B
T G T C C T N C T G G G G
c.448C>T
C
C1
C2
P
SUCLG1
β-TUBULIN
D
P1
P2
C1
C2
SUCLA2
β-TUBULIN

Figure 5